OPEN

Citation: Cell Death and Disease (2013) 4, e732; doi:10.1038/cddis.2013.257

www.nature.com/cddis

Glucose starvation induces cell death in K-ras-transformed cells by interfering with the hexosamine biosynthesis pathway and activating the unfolded protein response

This article has been corrected since Online Publication and a corrigendum has also been published

R Palorini[1,2], FP Cammarata[3], C Balestrieri[2,6], A Monestiroli[2], M Vasso[1,4], C Gelfi[1,4,5], L Alberghina[1,2] and F Chiaradonna*[,1,2]

Cancer cells, which use more glucose than normal cells and accumulate extracellular lactate even under normoxic conditions (Warburg effect), have been reported to undergo cell death under glucose deprivation, whereas normal cells remain viable. As it may be relevant to exploit the molecular mechanisms underlying this biological response to achieve new cancer therapies, in this paper we sought to identify them by using transcriptome and proteome analysis applied to an established glucose-addicted cellular model of transformation, namely, murine NIH-3T3 fibroblasts harboring an oncogenic *K-RAS* gene, compared with parental cells. Noteworthy is that the analyses performed in high- and low-glucose cultures indicate that reduction of glucose availability induces, especially in transformed cells, a significant increase in the expression of several unfolded protein response (UPR) hallmark genes. We show that this response is strictly associated with transformed cell death, given that its attenuation, by reducing protein translation or by increasing cell protein folding capacity, preserves the survival of transformed cells. Such an effect is also observed by inhibiting c-Jun NH2-terminal kinase, a pro-apoptotic signaling mediator set downstream of UPR. Strikingly, addition of *N*-acetyl-D-glucosamine, a specific substrate for the hexosamine biosynthesis pathway (HBP), to glucose-depleted cells completely prevents transformed cell death, stressing the important role of glucose in HBP fuelling to ensure UPR attenuation and increased cell survival. Interestingly, these results have been fully recognized in a human model of breast cancer, MDA-MB-231 cells. In conclusion, we show that glucose deprivation, leading to harmful accumulation of unfolded proteins in consequence of a reduction of protein glycosylation, induces a UPR-dependent cell death mechanism. These findings may open the way for new therapeutic strategies to specifically kill glycolytic cancer cells.
Cell Death and Disease (2013) **4,** e732; doi:10.1038/cddis.2013.257; published online 18 July 2013
Subject Category: Cancer Metabolism

Remodeling of energy metabolism is a recognized hallmark of cellular transformation that supports the sustained proliferation of cancer cells under conditions that restrict normal cell growth.[1,2] Hence, cancer cells rely mostly on glycolysis for ATP production as compared with parental normal cells that use mainly oxidative phosphorylation (OXPHOS).[3,4] The shift of energy metabolism to aerobic glycolysis is driven both by environmental growth conditions and by oncogenic mutations of protoncogenes and tumor-suppressor genes.[5,6] Impaired mitochondrial function is another important feature of transformed cell metabolic reprogramming.[2,3,7] In conditions of limited glucose availability, highly proliferating glucose-addicted cancer cells lose their enhanced growth ability and, finally, die.[8] Different processes are associated with and may contribute to the death of transformed cells in glucose deprivation, including ATP level decrease, radical oxygen species (ROS) accumulation and generally mitochondrial dysfunction.[9–11] Once triggered, these processes may induce cell death by activating a mitochondrial apoptotic route, through regulation of Bcl-2 homology 3-only

[1]SYSBIO, Centre of Systems Biology, Piazza della Scienza 2, Milano 20126, Italy; [2]Department of Biotechnology and Biosciences, University of Milano-Bicocca, Piazza della Scienza 2, Milano 20126, Italy; [3]LATO-HSR G.Giglio, contrada Pietrapollastra Pisciotto, Cefalù 90015, Italy; [4]Institute of Bioimaging and Molecular Physiology, National Research Council, via F lli Cervi 93, Segrate 20090, Italy and [5]Department of Biomedical Sciences for Health, University of Milan, via F lli Cervi 93, Segrate 20090, Italy

*Corresponding author: F Chiaradonna, SYSBIO, Centre of Systems Biology, Piazza della Scienza 2, 20126 Milano (MI), Italy or Department of Biotechnology and Biosciences, University of Milano-Bicocca, Piazza della Scienza 2, Milano 20126, Italy. Tel: +39 02 64483526; Fax: +39 02 64483552; E-mail: ferdinando.chiaradonna@unimib.it

[6]Current address: Department of Experimental Oncology, European Institute of Oncology (IEO), Via Adamello 16, 20139 Milan, Italy.

Keywords: cancer cell metabolism; glucose depletion; unfolded protein response; hexosamine biosynthesis pathway; cancer cell death

Abbreviations: CHOP, C/EBP homology protein; CHX, cycloheximide; eIF2α, eukaryotic initiation factor 2α; ER, endoplasmic reticulum; GlcNAc, *N*-acetyl-D-glucosamine; Grp78, glucose-regulated protein 78; HG, high glucose; HBP, hexosamine biosynthesis pathway; IRE1, inositol-requiring enzyme 1; JNK, c-Jun NH2-terminal kinase; LG, low glucose; OXPHOS, oxidative phosphorylation; PBS, phosphate buffer saline; PCA, principal component analysis; PERK, double-stranded RNA-activated protein kinase-like ER kinase; PI, propidium iodide; ROS, radical oxygen species; siRNA, small interfering RNA; TOF, time-of-flight; UPR, unfolded protein response; XBP1, X box-binding protein 1; 2-DIGE, two-dimensional difference gel electrophoresis; 4-PBA, 4-phenylbutyrate

Received 19.12.12; revised 06.6.13; accepted 10.6.13; Edited by C Munoz-Pinedo

proteins, by activating a caspase-8-dependent apoptotic process or by inducing necrosis.[12–14] As the glucose-dependent mechanism of cancer cell death may provide a useful target through which apoptosis may be induced in tumors while sparing healthy normal tissues, we sought to study glucose withdrawal and associated cell death in two different transformed cell lines. We used NIH-3T3 fibroblasts harboring an oncogenic *K-RAS* gene (G12V; transformed) compared with parental immortalized NIH-3T3 cells (normal) and a human breast cancer cell line, MDA-MB-231, carrying an oncogenic *K-RAS* gene (G13D) as well.[15] It is worth mentioning that both transformed cell lines, displaying a typical Warburg effect, are strongly sensitive to glucose exhaustion as, in such a condition, they show a strong increase in cell death.[10,16]

Glucose deprivation, as well as the treatment with the glucose analog 2-deoxy-D-glucose, has also been reported to activate the unfolded protein response (UPR), especially in cancer cells.[17] UPR is a cellular response to protein folding alteration orchestrated by different effectors[18] that may lead either to cell survival or to cell death depending on the strength and duration of the stimulus.[19] Under physiological conditions, 1–3% of intracellular glucose is shunted from the glycolytic pathway to the hexosamine biosynthesis pathway (HBP),[20] and flux through the HBP is mainly modulated on glucose availability but also requires glutamine, acetyl-coenzyme A and uridine triphosphate. The main product of HBP is uridine diphosphate-*N*-acetyl-D-glucosamine (GlcNAc), an important donor molecule for post-translational modifications, such as *N*- and *O*-glycosylation.[21] Although altered glycosylation via the HBP, especially N-linked glycosylation, upon 2-deoxy-D-glucose treatment[22] is reported to disrupt key cellular processes and to accumulate unfolded proteins,[23,24] the potential role of the HBP in glucose shortage-induced endoplasmic reticulum (ER) stress in cancer cells has not been fully elucidated.

In this report, starting from transcriptomic and proteomic data, we identified the relevant role of HBP and UPR activation in the route leading to cancer cell death upon glucose shortage. In fact, reduction of UPR activation significantly decreases cancer cell death upon glucose withdrawal. Moreover, UPR activation appears to depend on the reduction of protein glycosylation given that addition of GlcNAc totally prevents transformed cell death, indicating that prolonged impairment of protein folding is able to switch UPR from a protective to a harmful mechanism, especially in glucose-addicted cancer cells.

Results

Glucose starvation-induced death of transformed cells is associated with large transcriptional changes. To investigate the cell death mechanisms of transformed cells, induced by progressive glucose depletion, we performed a time-course transcriptional analysis (between 0 and 72 h) in normal and transformed cells grown under optimal conditions (high glucose (HG), 25 mM as initial concentration of glucose in the growth medium) or under glucose-limiting conditions (low glucose (LG), 1 mM as initial concentration of glucose; Figure 1a). The time interval was chosen because in LG the two cell lines, concurrently to the presence of residual glucose in the medium until 72 h, proliferate at almost the same rate[10,11] (Supplementary Figure 1). Afterwards, with the full glucose withdrawal, they display completely different behavior. Normal cells, starting from 72 h, undergo a contact-dependent inhibition as observed in HG (Supplementary Figure 1). In contrast, transformed cells in LG show an early decrease in the slope of the growth curve as compared with HG and a substantial increase in cell death between 72 and 96 h[10,11] (Supplementary Figure 1).

The results of the transcriptional analysis allowed the identification of 5925 statistically significant mRNAs whose expression changed along the time course (Figure 1b and Supplementary Table 1). Hierarchical clustering of these selected mRNA (Figure 1b) showed marked differences between HG and LG in transformed cells as well as in comparison with normal cells. Since the largest differences in gene expression were observed at the last analyzed time point (72 h), we decided to identify and use for further analyses those genes whose expression levels changed between 0 h and 72 h. These analyses identified 2049 modulated genes in normal cells in HG -NHG-, 1593 in normal cells in LG -NLG-, 1734 in transformed cells in HG -THG- and 1712 in transformed cells in LG -TLG-. Pathway enrichment analysis of these differentially expressed genes resulted in the identification of 64 pathways for NHG, 19 for NLG, 11 for THG and 39 for TLG (Figure 1c and Supplementary Table 2). As shown in Figure 1c, in NHG, among the most significant pathways, several wide-ranging cellular processes were identified such as that associated with DNA, RNA and protein metabolism, signaling pathways and cell cycle regulation. In contrast, in THG only a few of these pathways were identified (Figure 1c and Supplementary Table 2). Pathway analysis in LG growth indicated a different transcriptional response to glucose depletion of the two cell lines. In fact, only 11 of 39 pathways identified in transformed cells were shared with normal cells. In NLG, enriched pathways were almost the same as those observed in NHG (Figure 1c and Supplementary Table 2). Conversely, TLG showed enrichment of specific pathways involved in cell remodeling (i.e., *focal adhesion*, *cytoskeletal regulation by Rho GTPase*), cell metabolism (i.e., *cholesterol biosynthesis*, *biosynthesis of unsaturated fatty acids*), p53-related signaling and ER stress response (*protein processing in ER*; Supplementary Table 2).

Proteins differentially expressed between normal and transformed cells identify glycolytic enzymes and proteins involved in stress response. To further characterize transformed cells' specific signatures, cellular extracts from normal and transformed cells grown in HG and LG for 72 h were subjected to proteomic analyses by 2D difference gel electrophoresis (2-DIGE) coupled with mass spectrometry (Supplementary Figure 2). Comparing the two cell lines, we identified 41 proteins differentially expressed in NHG (N72HG) *versus* THG (K72HG) and 29 in NLG (N72LG) *versus* TLG (K72LG; Supplementary Table 3). These proteins were classified by their annotated function on the KEGG pathway. As shown in Supplementary Table 4, the differentially expressed proteins were almost the same in both glucose availabilities and were involved in *glycolysis,*

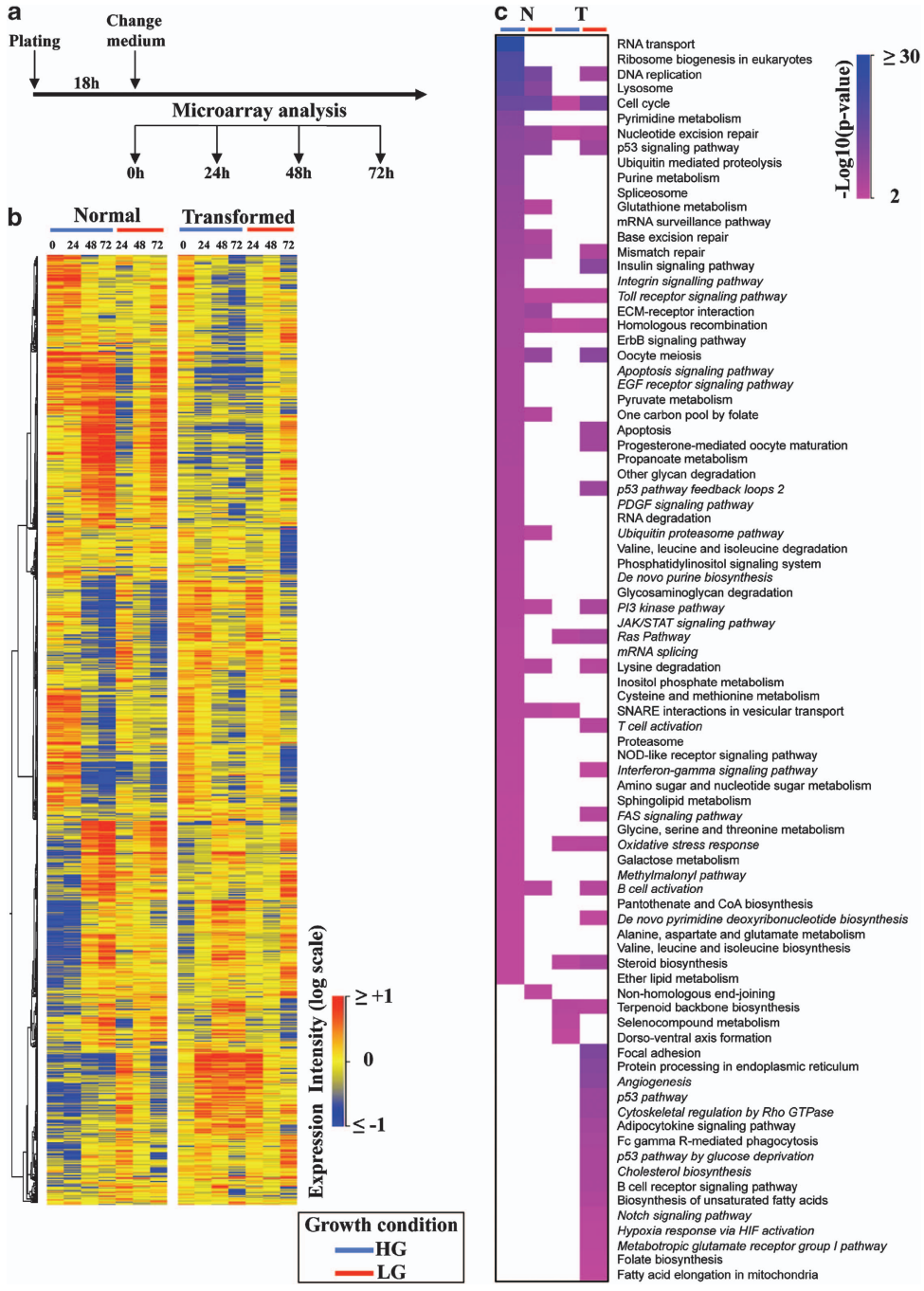

Figure 1 Genes and pathways regulated in normal and transformed cells grown in HG and LG. (**a**) Schematic representation of the experimental procedure used to identify regulated genes in both cell lines grown along a time course of 72 h and in two glucose concentrations. (**b**) Starting from 5295 genes identified by Welch's ANOVA and PCA, a hierarchal clustering was performed. Expression levels are depicted by a color log scale from red (high expression) to blue (low expression). Each row indicates the expression value of a transcript in a specific condition (columns). (**c**) Pathway enrichment analysis, according to their *P*-values, of the differentially expressed genes achieved at 72 h in both cell lines grown in HG and LG. The pathways have been ranked according to normal cells grown in HG

protein folding and synthesis and stress response. The latter process, however, was more modulated in TLG sample since the proteins related to this process were either specifically expressed (i.e., HSP90B1, PSMA1 and PRDX6) or more largely expressed (i.e., ESD, GSTO, SOD2 and PRDX1) in this condition, indicating the activation of a stress response under glucose depletion.

Gene network of ER stress in HG and LG. As the two analyses identified cellular processes associated with protein folding, cellular stress and ER stress, and as the latter is a regulated process that involves resident ER proteins, often induced at mRNA level by ER stress in a feedback loop, and a large set of downstream target genes,[24] we sought to identify ER stress-associated mRNAs in our transcriptional

profiles. This analysis allowed the identification of 57 genes encoding for proteins strictly associated with ER function, in control and stress conditions, and 59 UPR responsive genes, encoding for proteins regulating *survival*, *cell death* and other cellular processes indicated as *miscellaneous*. The 57 mRNAs, represented as colored ellipses (see legend) were used to generate an ER network (Figures 2a and b) composed of five key functional ER response sub-networks, shown in the figures as dotted line boxes, namely, *translation/translocation*, *unfolded protein binding*, *quality control*, *ER-associated degradation* and *translocation block*, respectively. The ER stress response was activated in cells grown in LG (Figure 2a), given that in HG (Figure 2b) the vast majority of these mRNAs were expressed at normal levels (yellow and light green color). Transformed cells grown in LG as compared with normal cells showed a significant number of upregulated mRNAs that are, for instance, mainly involved in reducing the loading of misfolded proteins and/or increasing folding activity, namely, *translation/translocation*, *unfolded protein binding* and *quality control.* In transformed cells, several ER stress genes were more upregulated, for instance some key regulators of UPR as *Hspa5*, also commonly known as *BiP or Grp78*, *Dnajc3*, commonly known as *p58IPK* and *Atf4*, suggesting a stronger activation of ER response as compared with normal ones. Analysis of the 59 downstream mRNAs (Figure 2c, Target mRNAs) confirmed an overall ER stress activation upon LG growth condition. However, although in transformed cells these mRNAs appeared to be differentially expressed between the two glucose conditions, in normal cells they were more similarly expressed, suggesting, for this cell line, a glucose-independent transcriptional regulation. Interestingly, in transformed cells grown in LG, several mRNA encoding for cell death-associated proteins were only slightly modulated (*Bid*,[25,26] *Parp1* and *Caspase12)* or even downregulated (*Calpain1* and *Bak*). In contrast, survival genes such as *Bcl2*, *Akt3 and Hyou1*[27,28] were upregulated. Overall, these findings confirmed the activation of an ER stress response, namely, UPR, in a glucose-dependent manner, and they also suggest a cell death mechanism partially independent of gene expression changes.

Experimental validation of UPR induction at mRNA and protein levels in normal and transformed cells. To investigate the transcriptional regulation of the UPR detected in the Affymetrix GeneChip data, we selected eight UPR target genes of which six were present (*Grp78*, *Atf4*, *XBP1*, *CHOP*, *CAR6* and *Trb3*) and two were absent (*GADD34* and *PDIa3*) in our transcriptional data, to assess their expression at 72 h both in HG and LG. Both cell lines, in agreement with the transcriptional data and as confirmed by RT-PCR, showed an increased expression of these genes only in LG (Figures 3a and b). Interestingly, the ER stress-dependent splicing of XBP1 (X box-binding protein) was detectable only in transformed cells (Figure 3a, right box). Further confirmation of UPR activation was obtained by western blot analysis to monitor glucose-regulated protein 78 (Grp78) and C/EBP homology protein (CHOP) levels, as UPR activation hallmarks. As expected, the expression of the two proteins was elevated in LG at 72 h (Figure 3b), whereas there was no evidence of expression of UPR proteins in cells grown in HG (Supplementary Figure 3).

Attenuation of protein translation or increase in cell folding capacity reduces UPR activation and transformed cell death. Experiments presented in the following provide clear evidence that the ability to attenuate translation or to increase protein folding in response to ER stress has an important role in mitigating the consequences of this insult on cell survival.[17,29] In fact, 24 h/48 h treatment with cycloheximide (CHX), a known protein synthesis inhibitor, or 4-phenyl butyrate (4-PBA), a chemical chaperone,[30,31] between 72 h and 96 h/120 h, rescued transformed cells from death in LG, as indicated by their proliferation (Figures 4b–d and Supplementary Figure 4B and C) and by Annexin V/propidium iodide (PI) analysis (Figures 4g and h and Supplementary Figure 4D and E). Importantly, neither treatment affected normal cell growth (Figures 4a–c and Supplementary Figure 4A) and survival (Figures 4e and f) as the percentage of cell death was almost comparable in all four samples. CHX and 4-PBA treatments also induced ER stress attenuation as confirmed by the strong reduction of UPR activation markers, Grp78 and CHOP (Figures 4i and j). A relation between CHOP expression and transformed cell death was confirmed through CHOP silencing by small interfering RNA (siRNA), which attenuated caspase 3 cleavage, as after treatment with CHX and 4-PBA (Supplementary Figure 5).

Glucose deprivation induces ER stress c-Jun NH2-terminal kinase (JNK)-mediated cell death specifically in transformed cells. The UPR relieves the ER stress by several mechanisms.[32] However, when the ER stress is prolonged or the adaptive response fails, apoptotic cell death ensues.[33,34] Among the different mechanisms activated by UPR to induce cell death, there is the activation of JNK through the IRE1-XBP1 UPR branch.[35] To explore a possible role of JNK activation in glucose deprivation-induced cell death, we measured the JNK phosphorylation, indicative of its activation. Upon glucose deprivation, JNK phosphorylation substantially increased in transformed cells (Figures 5a and b). Importantly, its inhibition, obtained by treatment with the specific inhibitor SP600125,[36] induced transformed cell survival (Figures 5d and f). Consistently, 4-PBA and CHX induced JNK inhibition (Figure 5h).

Figure 2 The ER networks for normal and transformed cells grown in LG (**a**) and in HG (**b**), derived by using mRNA expression data at 72 h, are presented. Each mRNA is represented by a colored ellipse; in particular, the external ellipse represents normal cell data and the internal ellipse transformed cell data. Changes in gene expression levels are represented by a color log scale from red (high expression) to blue (low expression). Unchanged level of expression (yellow) has been considered when mRNA had a value between -0.5 and 0.5. The double-color triangle below the regulated processes indicated the relation between time and intensity of ER stress and effect on cell homeostasis (blue survival, red death). (**c**) Hierarchical clustering of 58 known UPR target genes. UPR-related genes have been identified in our transcriptional analysis and their 72 h values for normal and transformed cells grown in HG and LG have been clustered

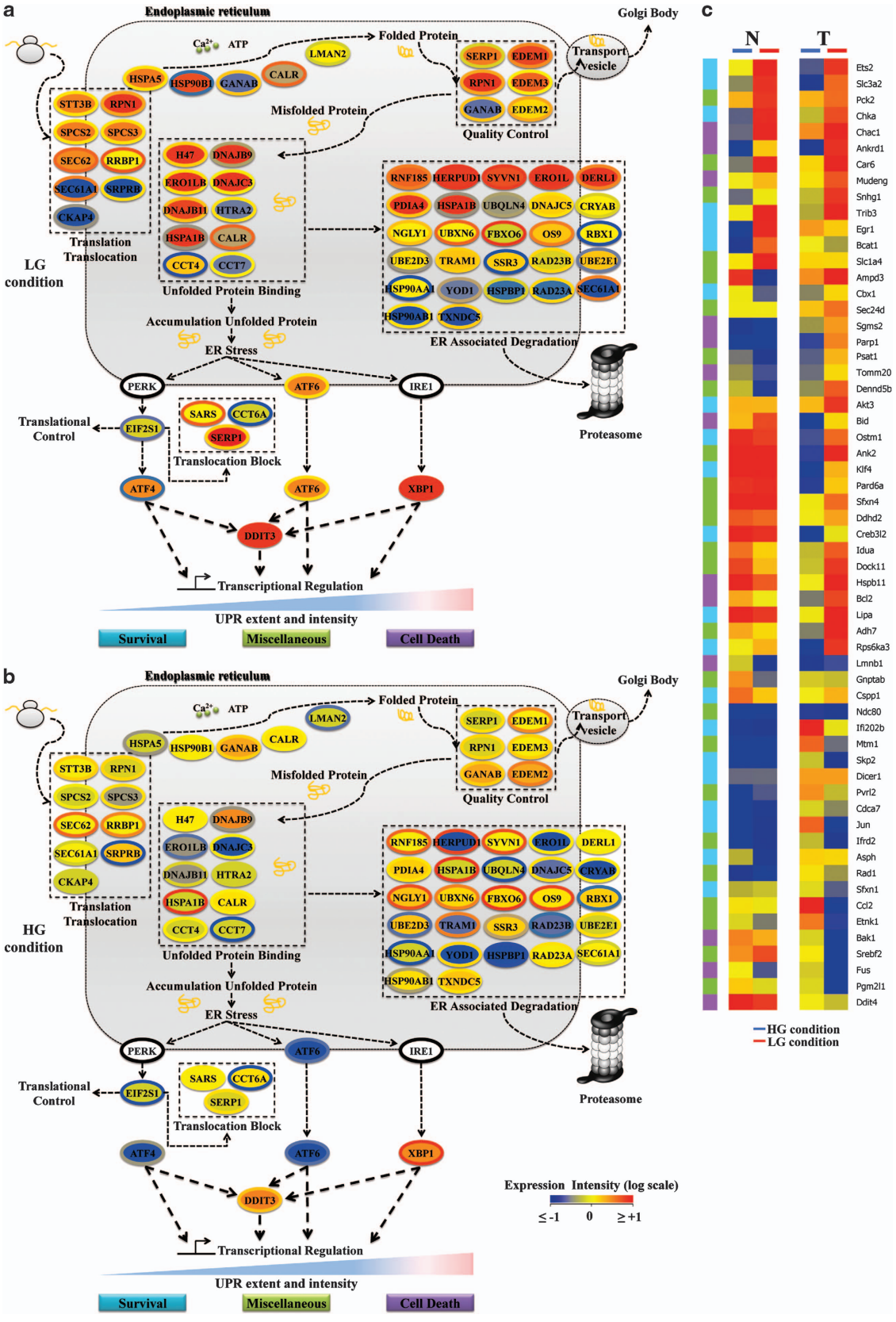
a
Endoplasmic reticulum
Golgi Body
Folded Protein
Transport Vesicle
Misfolded Protein
Quality Control
Translation Translocation
LG condition
Unfolded Protein Binding
Accumulation Unfolded Protein
ER Stress
ER Associated Degradation
Proteasome
PERK
ATF6
IRE1
Translational Control
Translocation Block
ATF4
XBP1
DDIT3
Transcriptional Regulation
UPR extent and intensity
Survival
Miscellaneous
Cell Death
b
HG condition
c
N
T
HG condition
LG condition
Expression Intensity (log scale)
≤-1
0
≥+1

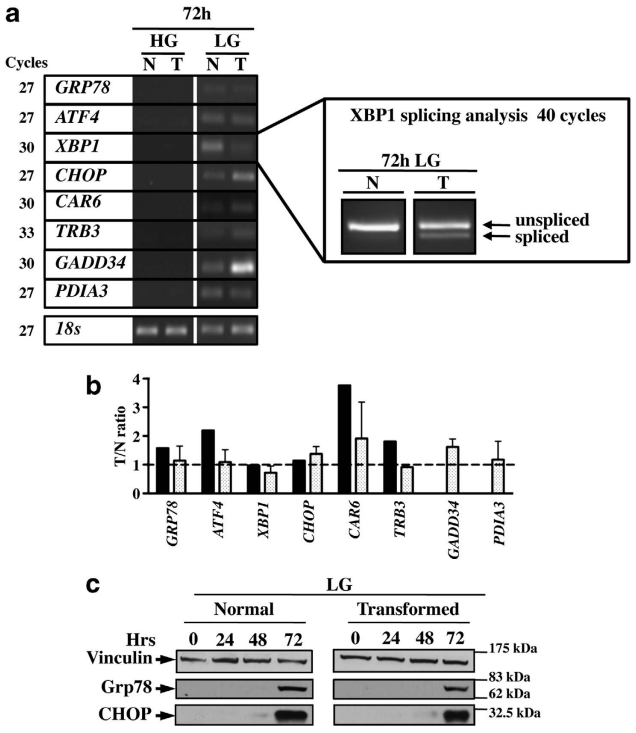

Figure 3 Semi-quantitative RT-PCR and western blot analysis indicated that UPR is activated at LG. (**a**) Semi-quantitative RT-PCR of the mRNAs specific for different UPR-related genes in normal (N) and transformed cells (T) at 72 h in HG and LG. (**b**) Comparison between the relative levels of expression calculated by Affymetrix and semi-quantitative RT-PCR for the same genes at LG. (**c**) Western blot analysis of UPR activation upon glucose depletion. To follow UPR activation, the expression of Grp78 and CHOP proteins was analyzed. Images are representative of at least three independent experiments

No effect on JNK activation was observed in normal cells in any of the analyzed conditions (Figures 5c, e and g). Taken together, these findings indicated that JNK activation by UPR has a role in glucose deprivation-induced transformed cell death.

GlcNAc addition upon glucose depletion rescues transformed cell survival by reducing UPR. As glucose deprivation induced a pronounced expression of UPR marker genes, especially in transformed cells, we sought to determine whether this activation was a consequence of a reduced precursor entry into HBP and hence a reduction of *N*- and *O*-protein glycosylation that ultimately leads, in the case of *N*-glycosylation reduction, to unfolded protein accumulation.[37,38] We assayed normal and transformed cells for alterations in protein *O*-GlcNAcylation, as a marker of HBP flux reduction, in response to changes in glucose concentration. Normal cells presented a time- and glucose-dependent decrease in *O*-GlcNAc protein modification levels (Figures 6a and c).In both glucose concentrations and at all analyzed time points, transformed cells showed a higher level of *O*-GlcNAc as compared with normal cells. Moreover, a severe reduction of *O*-GlcNAc was observed in LG as compared with HG (Figures 6b and d). These data indicated that in transformed cells, and to a lesser extent in normal cells, the level of *O*-GlcNAc is dependent upon glucose availability, as its shortage induces a glycosylation decrease that finally may lead to UPR activation.

Hence, we evaluated whether the addition of GlcNAc affected ER stress-induced transformed cell death under glucose depletion. Given that GlcNAc can fuel the HBP without contributing significantly to glycolysis,[39] this addition allowed us to ascertain whether stimulation of HBP was sufficient to promote UPR attenuation and cell survival. To confirm that GlcNAc entered HBP, we evaluated *O*-GlcNAcylation protein status after treatment with the molecule. Both cell lines presented a GlcNAc concentration-dependent change of *O*-glycosylation pattern (Supplementary Figure 6). 24 h/48 h treatment with GlcNAc between 72 h and 96 h/120 h, whereas it did not affect the proliferation of normal cells (Figure 6e and Supplementary Figure 7A), rescued transformed cell survival in a dose-dependent manner (Figure 6f and Supplementary Figure 7B and C). Nevertheless, in both cell lines a dose-dependent decrease in the expression of Grp78 and CHOP upon GlcNAc treatment, like in the glucose-replaced samples (Glc), was observed (Figure 6g and h). In agreement with these results, Annexin V/PI staining (Figures 6i and j) after 10 mM GlcNAc treatment showed a protective effect in both cell lines, which was more consistent in transformed cells. Accordingly, the GlcNAc treatment also induced a prolonged JNK inhibition specifically in transformed cells (Figure 6k and l and Supplementary Figure 7D).

GlcNAc protects glycolytic human cancer cells MDA-MB-231 from glucose-dependent cell death. Our findings indicate that glucose deprivation, leading to a reduced HBP flux, prolongs UPR activation, most likely as a consequence of accumulation of unfolded proteins, and hence cell death. In order to evaluate whether this mechanism was also effective in a glucose-addicted human cancer cell line, namely, MDA-MB-231, we tested UPR activation in these cells grown for 96 h in LG as compared with HG. As shown in Figure 7a, Grp78 and CHOP protein levels increased only in LG, in correlation with the complete glucose depletion from culture medium[40] (data not shown). In association, caspase 3 activation and anti-apoptotic protein Bcl-2 reduction were observed (Figure 7a), suggesting that glucose-depleted cells were progressing to cell death. Next, we evaluated the effect of GlcNAc addition to cells. As an early activation of UPR was observed in these cells, we decided to treat the cells between 48 h and 72 h. GlcNAc increased cell survival (Figures 7b and c) and led to a clear decrease in the two UPR markers, in JNK and caspase 3 activation, as well as to a slight increase in Bcl-2 expression (Figure 7d), confirming that the treatment was able to attenuate UPR and protect cells from apoptosis. JNK inhibition induced an increase in cell survival (Figures 7e and f), associated with a significant decrease in caspase 3 activation (Figure 7g), further confirming the role of this kinase in UPR-mediated MDA-MB-231 cell death.

Discussion

Cell death upon glucose deprivation occurs in several cancer cells and is associated with a number of molecular events including ATP level fall, ROS accumulation and mitochondrial

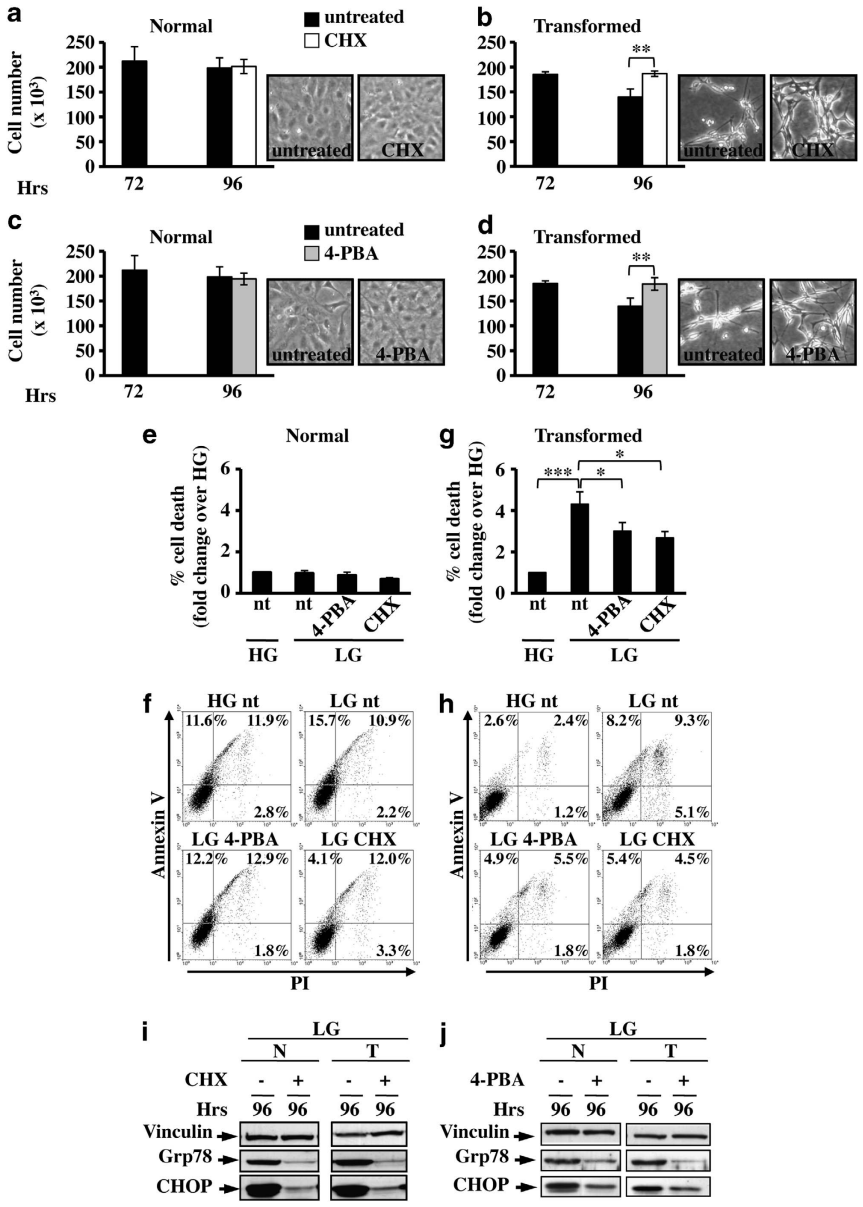

Figure 4 Attenuation of UPR by cycloheximide (CHX) or sodium 4-phenylbutyrate (4-PBA) protects transformed cells from death. Cell death and UPR activation were analyzed in normal and transformed cells grown in LG for 72 h and treated for the further 24 h with CHX or 4-PBA. Normal (**a** and **c**) and transformed (**b** and **d**) cells were counted at 72 h and 96 h, after treatment with CHX (**a** and **b**) or 4-PBA (**c** and **d**). Data represent the average of at least three independent experiments (± S.D.); $^{**}P<0.01$, Student's *t*-test. Phase contrast microscopy images of untreated and treated transformed cells at 96 h of culture are shown. (**e**–**h**) FACS analysis of normal (**e** and **f**) and transformed (**g** and **h**) cells stained with Annexin V-FITC and propidium iodide. The percentage of cell death for normal and transformed cells was calculated considering Annexin V- and PI-stained cells alone and in combination; representative dot plots of normal (**f**) and transformed (**h**) cells are shown. Data represent the average of at least three independent experiments (± S.E.M); $^{*}P<0.05$, $^{***}P<0.001$, Student's *t*-test. UPR activation after CHX (**i**) and 4-PBA (**j**) treatments was followed through the expression analysis of Grp78 and CHOP proteins. Figures are representative of three independent experiments

dysfunction[9–11,41] (Figure 8a). Accordingly, our previous reports indicate that K-ras-transformed mouse and human cells upon glucose depletion undergo intracellular ATP-level decrease and accumulation of intracellular ROS as a consequence of mitochondrial complex I dysfunction and ultimately cell death.[9,11,16,42] Importantly, LG-cell death in both cancer cell lines is partly avoided by ROS level reduction or by enhancement of mitochondrial activity.[11] Nevertheless, the complete mechanism by which glucose depletion induces cancer cell death is not yet fully understood.

The present study had, as its first aim, the identification of changes in gene and protein expression induced by glucose deprivation in order to characterize the processes involved in transformed cell death. Our results indicate that glucose deprivation induces ER stress and hence UPR activation. Importantly, we show that such activation is due to a reduction of glucose entry into the HBP, which reduces proteins' glycosylation levels, as shown by alteration of *O*-glycosylation, and hence leads to a sustained UPR stimulation and to transformed cell death.

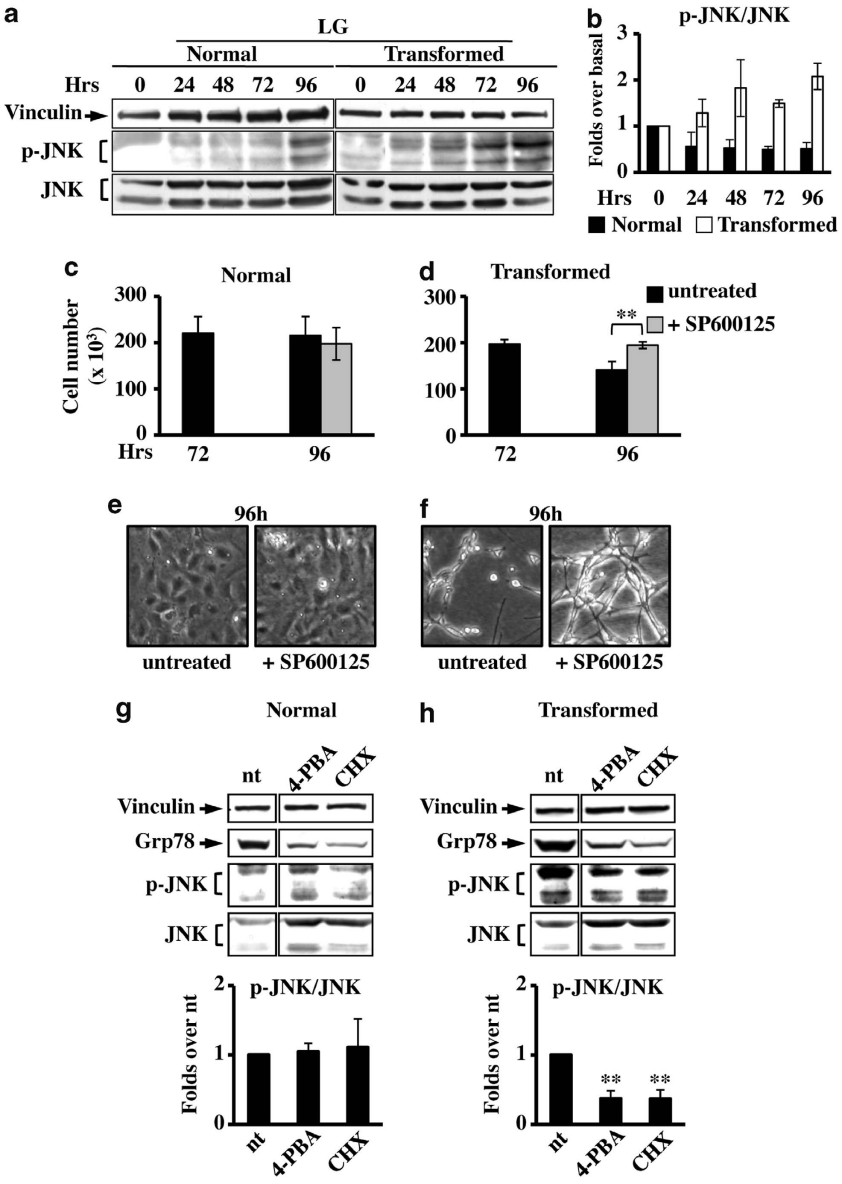

Figure 5 JNK inhibition causes survival in transformed cells grown in LG. (**a**) For JNK expression analysis, normal and transformed cells, grown in LG, were collected at indicated time points and total cellular extracts were subjected to SDS-PAGE followed by western blot analysis with antibodies anti-phospho-JNK Thr183/Tyr185 (p-JNK) and anti-total JNK. As loading control the expression of vinculin was analyzed. (**b**) Quantitative analysis of JNK phosphorylation status was performed by densitometric analysis of western blot films. The values obtained for P-JNK were normalized to the corresponding total JNK and vinculin values and plotted as fold changes over basal sample (0 h = 1). Normal (**c**) and transformed (**d**) cells, grown in LG, were counted at 72 h and 96 h after 24 h of treatment with the JNK inhibitor, SP600125. Phase contrast microscopy images were collected for untreated and treated normal (**e**) and transformed (**f**) cells at 96 h of culture. All data represent the average of at least three independent experiments (± S.D.); $^{**}P<0.01$, Student's *t*-test. (**g** and **h**) Analysis of p-JNK level in normal (**g**) and transformed (**h**) cells at 96 h of culture after 24 h of treatment with 4-PBA and CHX. The densitometric values for p-JNK, shown in the bottom histograms, were normalized as above and plotted as fold change over untreated (nt) sample. Data represent the average of at least three independent experiments (± S.E.M.); $^{**}P<0.01$ as compared with nt, Student's *t*-test. UPR activation was followed through the expression analysis of Grp78 and as loading control the expression of vinculin was used

Although the role of UPR is to reduce ER stress and induce survival (Figure 8b), persistent ER stress is known to cause cell death (Figure 8c).[18,43] Interestingly, our data show that UPR is activated in both normal and transformed cells, but that only normal cells are able to cope with this stress, avoiding massive cell death. We make the hypothesis that the concomitant presence in normal cells of low ROS levels, sustained ATP levels, mitochondria functionality[10,11,16] and a tunable UPR may provide the conditions necessary to re-establish cellular homeostasis (Figures 8a and b). Indeed, transcriptional data indicate a more sustained UPR activation in transformed cells as compared with normal cells, as several UPR-related genes and relative targets are more actively expressed in these cells (Figures 2 and 8c). In transformed cells the following are observed: XBP1 splicing (Figures 3 and 8c); GADD34 and P58IPK mRNAs expression (Figures 3 and 8c), whose induction may induce death by quickly restoring protein synthesis through their

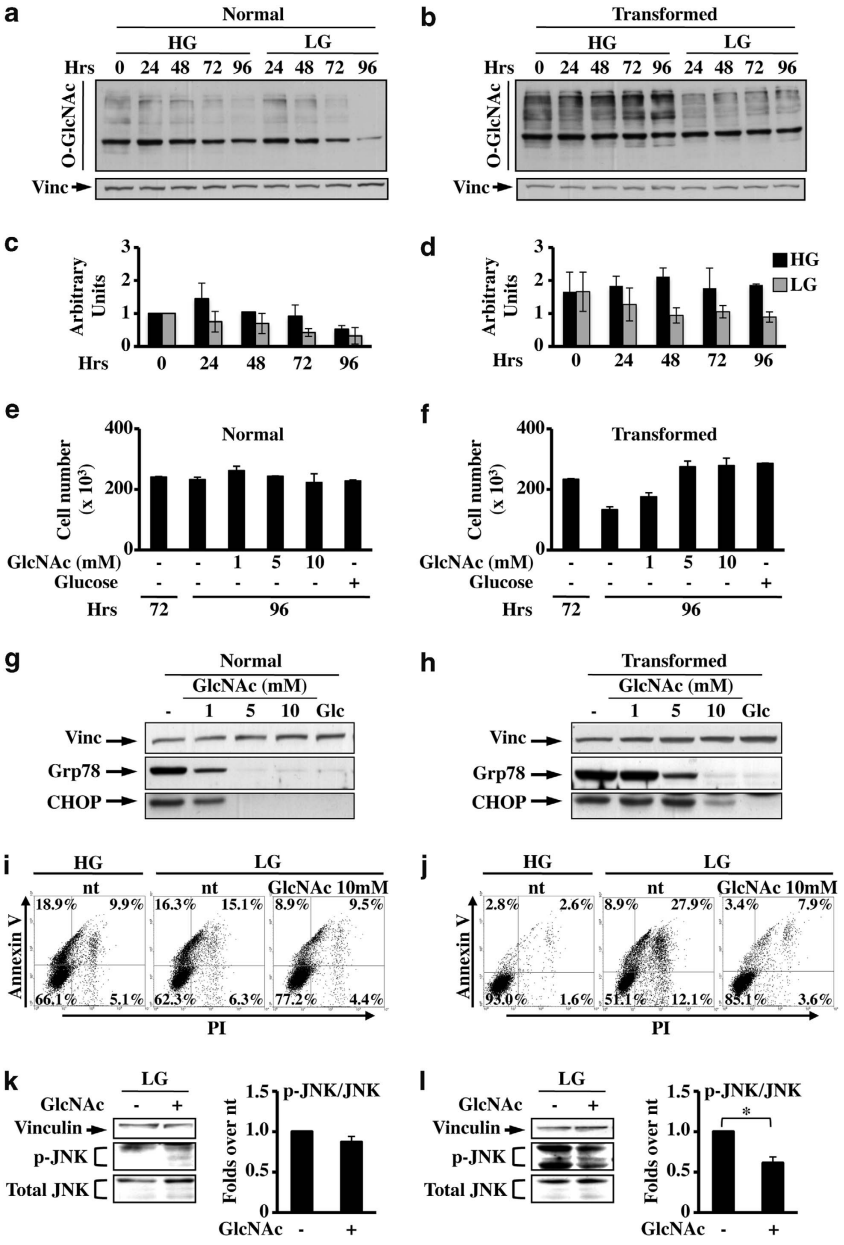

Figure 6 *N*-Acetyl-D-glucosamine (GlcNAc) protects transformed cells from glucose depletion-dependent cell death. Normal (**a**) and transformed (**b**) cells, grown in HG and LG, were subjected to western blot analysis with anti *O*-glycosylation antibody (*O*-GlcNAc). As loading control the expression of vinculin and Ponceau staining (data not shown) was analyzed. Quantitative analysis of *O*-glycosylation status was performed by densitometric analysis of western blot films of normal (**c**) and transformed (**d**) cells. The values obtained for *O*-GlcNAc were normalized to the corresponding vinculin values and plotted as fold change over the normal sample 0 h (0 h = 1) both in HG and LG. Normal (**e**) and transformed (**f**) cells, grown in LG, were counted at 72 and 96 h after 24 h of treatment with different concentrations of GlcNAc or 1 mM glucose. Data represent the average of at least three independent experiments (± S.D.). (**g** and **h**) UPR activation after GlcNAc or glucose (Glc) treatment was followed through the expression analysis of Grp78 and CHOP proteins. (**i** and **j**) FACS analysis of Annexin-V plus PI-labeled normal (**i**) and transformed (**j**) cells, grown until 96 h in HG (left panels), LG (middle panels) and LG + 10 mM GlcNAc (24 h of treatment). Figures are representative of three independent experiments. (**k** and **l**) Analysis of the expression of p-JNK in normal (**k**) and transformed (**l**) cells at 96 h of culture. The values obtained for p-JNK, shown in the right histograms, were normalized to the corresponding total JNK and vinculin values and plotted as fold changes over nt samples. Data represent the average of at least three independent experiments (± S.E.M.); $^{*}P < 0.05$, Student's *t*-test. As loading control the expression of vinculin was used

effect on phosphorylation status of eukaryotic initiation factor 2α (EIF2α) and double-stranded RNA-activated protein kinase-like ER kinase (PERK), respectively;[44–46] TRB3 mRNA expression, which induces apoptosis through its inhibitory effect on pro-survival kinase AKT (Figures 3 and 8c);[47,48] and ERO1L expression, which controls the apoptotic process by increasing ROS levels and potentiating calcium release.[49,50] In addition, transformed cells also show JNK kinase activation (Figures 5, 6, 7 and 8c) that induces cell death by inhibiting the anti-apoptotic function of Bcl-2 protein.[51–53] Taken together, these findings strongly support the notion that transformed cells growing in normoxia, upon glucose deprivation, undergo

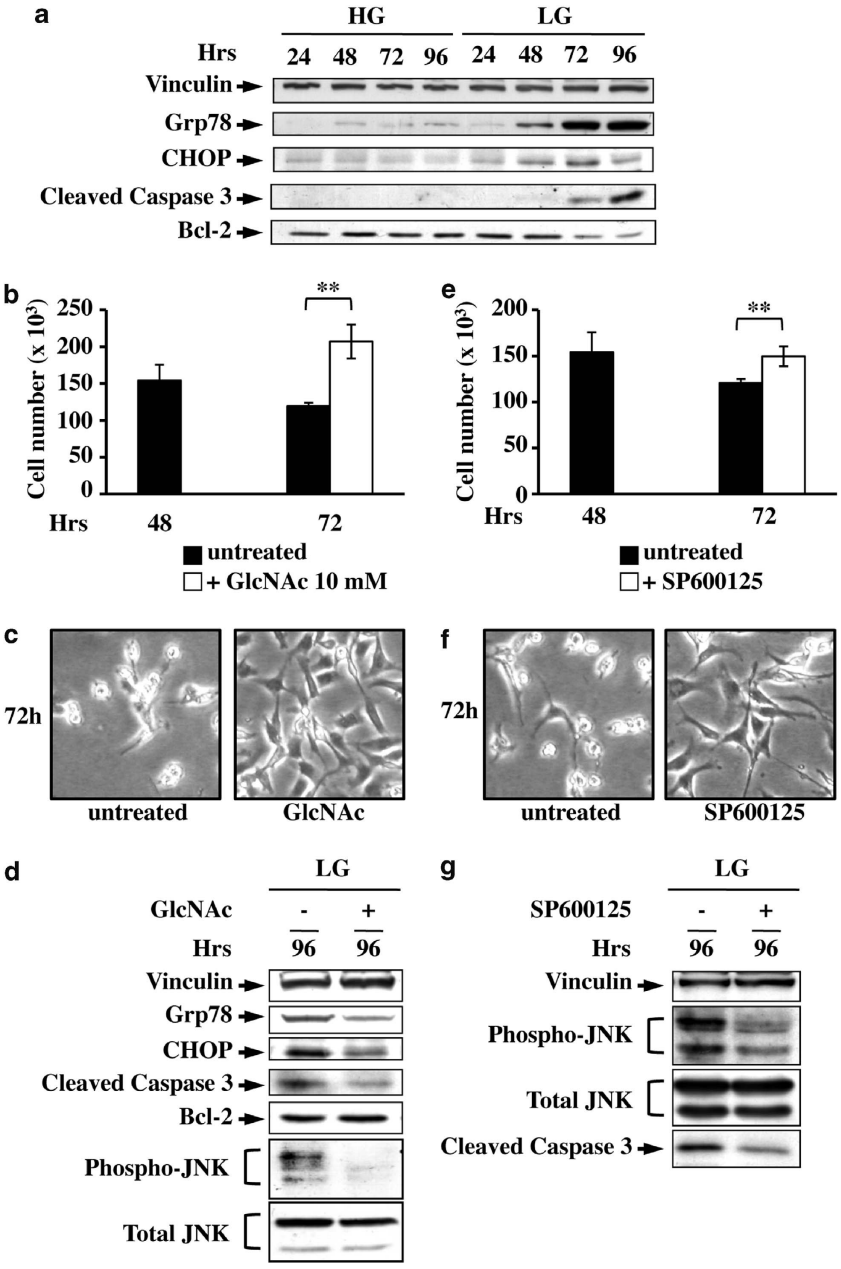

Figure 7 Glucose-addicted human cancer cells are protected from cell death by *N*-acetyl-D-glucosamine (GlcNAc) and JNK inhibitor. (**a**) Western blot analysis of UPR and cell death activation in MDA-MB-231 grown in HG and LG. To follow the UPR and cell death processes, the expression levels of Grp78 and CHOP as well as of cleaved caspase 3 and Bcl-2 were analyzed, respectively. MDA-MB-231 cell survival was analyzed by counting untreated cells at either 72 h of LG growth or after 24 h of treatment with 10 mM GlcNAc (**b**) or SP600125 (**e**). Data represent the average of at least three independent experiments (± S.D.); $^{**}P < 0.01$, Student's *t*-test. Phase contrast microscopy images were collected for untreated and treated (+ GlcNAc, **c**; + SP600125, **f**) cells at 72 h of culture. (**d**) UPR activation and cell death at LG and upon GlcNAc treatment were followed through the expression analysis of Grp78, CHOP, cleaved caspase 3, Bcl-2 and p-JNK. (**g**) JNK inhibitor effect on cell survival was followed by western blot analysis of JNK phosphorylation, as control, and caspase 3 activation. Figures are representative of three independent experiments

cell death through prolonged UPR activation due to unfolded protein accumulation. Indeed, as shown in Figure 8d, attenuation of UPR, obtained by decreasing unfolded protein accumulation (CHX), increasing cell folding ability (4-PBA) or inhibiting a downstream pro-apoptotic signaling (JNK inhibitor SP600125), protects transformed cells from glucose-dependent death. Moreover, our results show for the first time that HBP fueling by addition of GlcNAc, a sugar essential for *O*- and *N*-glycosylation, induces prolonged survival of glucose-deprived K-Ras-transformed cells by inhibiting UPR activation, with a decrease in CHOP expression and JNK activation (Figures 6, 7 and 8d). The ability of GlcNAc to completely restore transformed cell survival in the absence of glucose provides strong evidence that HBP, regulating protein folding and localization through the synthesis of uridine diphosphate-GlcNAc, represents an important pathway sensitive to glucose deficiency that is upregulated during transformation.[54,55] Remarkably, mannose addition showed

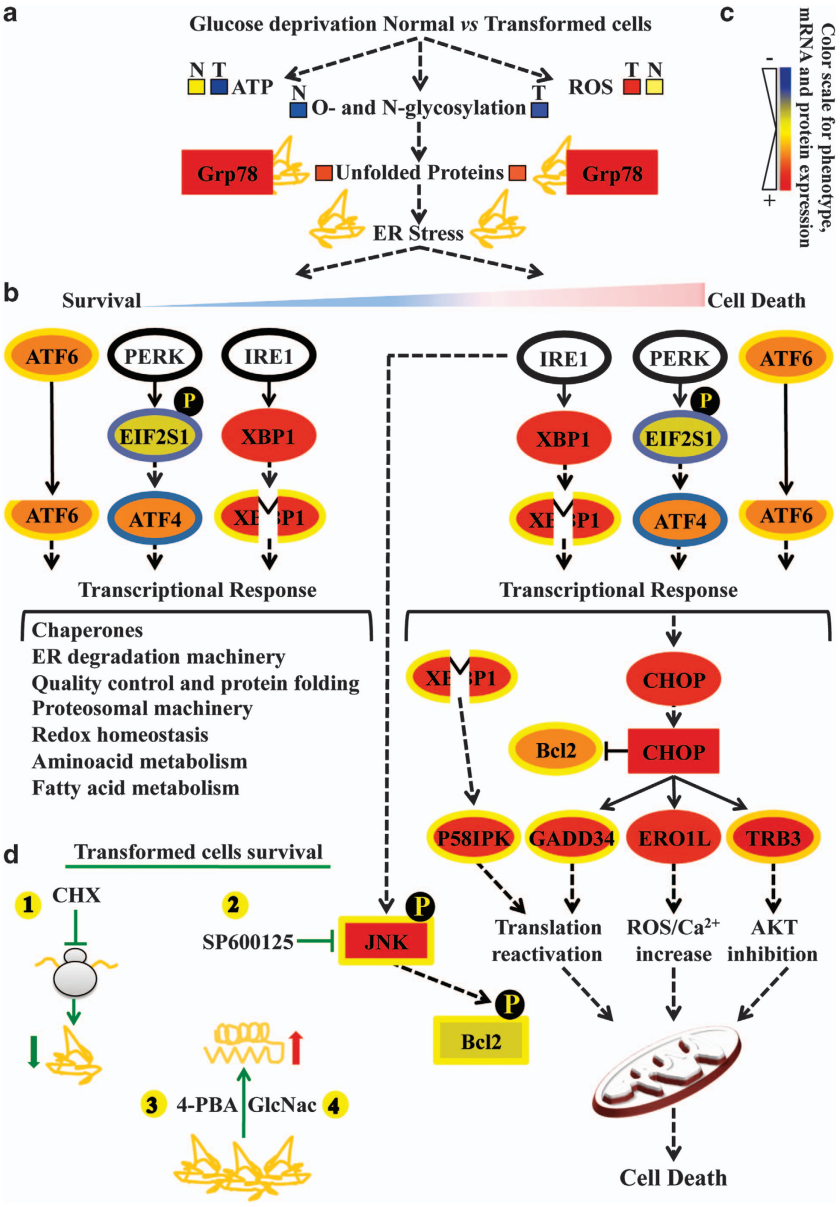

Figure 8 Glucose deprivation in cancer cells activates UPR following HBP flux reduction. Proteins are represented by a colored rectangle; in particular, the external rectangle represents normal cell data and the internal rectangle transformed cell data. Similarly, each mRNA has been represented by a colored ellipse, in which the external ellipse represents normal cell data and the internal ellipse transformed cell data. Changes in protein and gene expression levels are represented by a color scale between red (high expression) and blue (low expression); yellow indicates unchanged expression. Levels of ATP, ROS and unfolded proteins in normal (N) and transformed (T) cells (**a**) are represented by colored boxes. The double-color triangle in **a** under ER stress indicated the relation between time and intensity of ER stress and effect on cell homeostasis (blue: survival, red: death). (**b**) Survival processes activated by UPR have been represented as a cascade of events starting from UPR sensors activation (ATF6 cleavage, eIF2a phosphorylation, *EIF2S1* gene, by PERK, ATF4 expression and XBP1 splicing from expression upon IRE1 activity) and ending with a list of downstream regulated processes (transcriptional response). (**c**) The cell death process activated by UPR has been presented as a cascade of events starting from UPR sensor activation (as above) and ending either with a transcriptional response (*CHOP*, *P58IPK*, *GADD34*, *ERO1L*, *TRB3*) or a post-translational mechanism (phosphorylation) positively controlling JNK and negatively controlling Bcl-2 proteins. (**d**) Schematic representation of the transformed cells' survival mechanisms identified in our work. The protective effects of CHX (1, translation inhibition), SP600125 (2, JNK inhibitor), 4-PBA (3, chemical chaperone) and GlcNac (4, HBP substrate) are shown

similar results (data not shown). Overall, our findings are supported by literature data indicating that K-ras-expressing tumors increase glucose flux through a few metabolic pathways, among which HBP has an important role,[54] and that GlcNAc addition may induce normal hematopoietic cell survival, in the complete absence of glucose, by increasing membrane receptor localization, glutamine uptake and mitochondrial function.[39] Our results do not exclude the possibility that other processes, known to be either pro-survival or pro-apoptotic, for example, autophagy and mitochondrial dysfunction, could participate, together with HBP flux reduction and UPR activation, in determining a detrimental effect of glucose depletion on cancer cells. A deeper understanding of the HBP-UPR axis and its links with mitochondrial metabolism in relation to cancer cells is expected to open new avenues to therapeutic opportunities for cancer.

Materials and Methods

Cell culture and treatments. Mouse embryonic fibroblast NIH3T3 cells (obtained from the ATCC, Manassas, VA, USA), K-Ras-transformed NIH3T3-derived cell line 226.4.1[56] and MDA-MB-231 cells were routinely cultured in Dulbecco's modified Eagle's medium containing 4 mM L-glutamine, 100 U/ml penicillin and 100 mg/ml streptomycin (complete medium), supplemented with 10% newborn calf serum (mouse cells) or 5% fetal bovine serum (human cells). All reagents for media were purchased from Life Technologies (Carlsbad, CA, USA).

For the analyses, cells were plated at a density of 3000 cells/cm^2 in complete growth medium. After 16 h cells were washed twice with phosphate buffer saline (PBS) and incubated in growth medium (time 0) without glucose and sodium pyruvate (Life Technologies), supplemented with 25 mM (HG) or 1 mM (LG) glucose (Sigma-Aldrich Inc., St. Louis, MO, USA). Cells were then collected for further analyses at 24, 48, 72, 96 and 120 h of culture.

For specific treatments, 20 μM SP600125 (Santa Cruz Biotechnology Inc., Santa Cruz, CA, USA) or 35 μM CHX (Enzo Life Sciences Inc., Farmingdale, NY, USA) or 20 mM sodium 4-phenylbutyrate (Enzo Life Sciences) or 1–10 mM GlcNAc (Sigma-Aldrich) were added to the cells grown in LG at a specified time point of culture and the effects were analyzed 24/48 h later. Two hundred nanomolar thapsigargin (Adipogen, Liestal, Switzerland) was added for 6 h to cells grown in HG glucose.

To measure cell proliferation, harvested cells were counted using a Burker chamber.

PI/Annexin-V-FITC staining was performed using the Apoptosis kit from Immunological Science (Rome, Italy) and analyzed by FACScan flow cytometer (Becton-Dickinson, Franklin Lakes, NJ, USA) with CellQuest software (Becton-Dickinson). Flow cytometric data were then collected using WinMDI

D-Glucose measurement. D-Glucose levels in culture medium were determined using a spectrophotometric enzymatic assay kit (R-Biopharm, Darmstadt, Germany) as specified by the manufacturer's datasheet.

siRNA. The siRNA duplex for CHOP (siCHOP) was purchased from Sigma-Aldrich with the sequence as follows: 5′-GGAAGAACUAGGAAACGGA-3′. The negative control siRNA (siCTRL) was purchased from Qiagen (Hilden, Germany). The transfection of siRNA oligonucleotides was performed with ITERFERin siRNA transfection reagent (Polyplus transfection, New York, NY, USA) according to the manufacturer's datasheet. Briefly, for a 24-well plate siRNA was diluted in 100 μl of medium without serum and glucose and, after pipetting, 2 μl of ITERFERin were added. The mix was homogenized, incubated at RT for 10 min and added to the well, without changing the culture medium. After transfection, the final volume of medium in the well was 600 μl and the siRNA concentration was 80 nM.

Western blot analysis. For the analysis of protein levels, cells were harvested and disrupted in an appropriated lysis buffer. Thirty microgram of the total cellular extracts were then resolved by SDS-PAGE and transferred to the nitrocellulose membrane, which was incubated overnight with specific antibodies: vinculin, Grp78 and CHOP (GADD153) from Santa Cruz Biotechnology Inc.; phospho-JNK Thr183/Tyr185, total JNK and cleaved caspase 3 from Cell Signaling Technology Inc. (Danvers, MA, USA); Bcl-2 from Calbiochem (Merck Millipore, Darmstadt, Germany); and *O*-linked GlcNAc from Abcam (Cambridge, UK).

RNA extraction and semiquantitative RT-PCR analysis. RNA was extracted from cells cultured using Trizol reagent (Life Technologies). Total RNA was reverse-transcribed with oligo-dT by using the Superscript III RT-PCR First-Strand Synthesis System for RT-PCR (Life Technologies).

The RT product (0.2 μg) was amplified with primer pairs specific for the genes studied. As internal control of PCR assays, specific primers for 18S transcript were used.

Primers used: GRP78 forward: 5′-AGTGGTGGCCACTAATGGAG-3′, reverse: 5′-CAATCCTTGCTTGATGCTGA-3′; ATF4 forward: 5′-TCGAT GCTCTGTTTCGAATG-3′, reverse: 5′-GGCAACCTGGTCGACTTTTA-3′; XBP1 forward: 5′-CTGACGAGGTTCCAGAGGTG-3′, reverse: 5′-AGCAGACTCTGGG GAAGGAC-3′; CHOP forward: 5′-CATACACCACCACACCTGAAAG-3′, reverse: 5′-CCGTTTCCTAGTTCTTCCTTGC-3′; CAR6 forward: 5′-GCCCTCCATGTACCTT GAAA-3′, reverse: 5′-GACGGCTAACACAGCTAGGC-3′; TRIB3 forward: 5′-GATGC CAAGTGTCCAGTCCT-3′, reverse: 5′-CTTGCTCTCGTTCCAAAAGG-3′; GADD34 forward: 5′-AGGACCCCGAGATTCCTCTA-3′, reverse: 5′-CCTGGAATCAGGGG TAAGGT-3′; PDIA3 forward: 5′-TCTGAACCCATCCCAGAGTC-3′, reverse: 5′-GTGGCATCCATCTTGGCTAT-3′; 18S forward: 5′-GTTGGTGGAGCGAT TTGTCT-3′, reverse: 5′-GGCCTCACTAAACCATCCAA-3′.

Transcriptomic analysis

Affymetrix GeneChip processing: The cRNA was generated by using the Affymetrix One-Cycle Target Labeling and Control Reagent kit (Affymetrix Inc., Santa Clara, CA, USA), following the manufacturer's protocol. Total RNA was extracted from biological duplicate samples and analyzed using Affymetrix Genechips (Mouse Genome 430 2.0 Array) to determine the global gene expression patterns. The Mouse Genome 430 2.0 Array contains more than 45 000 probe sets including approximately over 34 000 well-substantiated mouse genes. Chips were washed and scanned on the Affymetrix Complete GeneChip Instrument System and processed into CEL files. The complete array data are available at the GEO database under accession GSE29962.

Affymetrix GeneChip data normalization and filtering: The data CEL files were imported, normalized and summarized as probe-level intensity measurements[57] by using the Robust Multi-array Average method and GeneSpring GX 11.5 software (Agilent Technologies). Starting from the perfect-match probe-level data of a set of arrays, this software performs the background correction and the normalization and finally summarizes the results as a set of expression measures for each probe set. Subsequently, 'per-gene normalization' was performed as described in GeneSpring's manual obtaining the absolute expression intensity as log2 scale. Moreover, CEL files were analyzed using the Affymetrix MAS 5.0 algorithm to obtain the flag data, which have been used to filter the Robust Multi-array Average-normalized data. Probe sets that receive absent calls are usually associated with low-intensity expression values and/or a high level of intra-probe set variability. Therefore, in order to reduce the contribution of noise-based error in subsequent statistical analysis, each probe set that did not receive at least two present calls across all 28 chips was removed ($\sim$50% of transcripts were selected).

Global gene profiling: All statistical analyses were performed using GeneSpring GX 11.5 software starting from filtered data. The principal statistical method used was Welch's one-way ANOVA (parametric test, variances not assumed to be equal) to identify individual genes with a dynamic expression across all time points, removing probe sets that exhibited no significant change in mean signal intensity (*P*-values cutoff 0.05). Because our primary aim in this report was to determine those genes with significant glucose deprivation-induced expression change, we also performed the principal component analysis (PCA) to determine whether a set of genes would separate from others with a significant interaction of treatment and time at 72 h (absolute correlation cutoff 0.90).

Subsequently, a probe set selection algorithm was carried out to select a representative probe set for each gene starting from all genes selected by ANOVA and PCA analysis. A probe set was rejected if its expression value was near to the background value (threshold beyond 0.5, log-scale) and if it hybridized with transcripts of two or more distinct genes. All the probe sets were then ranked with respect to their *P*-value and correlation value and the most significant one was selected as representative of the gene. These approaches have resulted in a list of 5295 unique modulated genes.

Cluster analysis: To cluster the temporal gene abundance, we used GeneSpring GX 11.5 software. We used absolute expression values (log-scale) for Hierarchical clustering employing the following parameters: Euclidean distance was set as similarity measure, Centroid was set as ordering function.

Proteomic analysis

Protein extraction: Cultured NIH3T3 normal and NIH3T3 transformed cells were washed twice with PBS and harvested in ice-cold PBS by scraping. After centrifugation at 800 $\times$ *g* for 10 min, the pellet was suspended in lysis buffer (7 M urea, 2 M thiourea, 4% CHAPS, 30 mM Tris and 1 mM PMSF), and solubilized by sonication on ice for proteomic analysis. Proteins were selectively precipitated using the 2-D-Clean up kit (GE Healthcare, Wauwatosa, WI, USA) in order to remove nonprotein impurities from samples, and re-suspended in lysis buffer. Protein extracts were adjusted to pH 8.5 by addition of 1 M NaOH. Protein concentration was determined with the 2-D-Quant kit (GE Healthcare).

2D DIGE: Protein labeling, 2D separation and image acquisition (for NIH3T3 normal and NIH3T3 transformed cells) were performed as previously described.[58]

Spot detection and statistically significant differences of 2D DIGE were performed using Progenesis SameSpot (Nonlinear Dynamics). For each gel undergoing the co-detection procedure, the estimated number of spots was set to 10 000, and filter parameters were set as follows: slope >1.2, minimal area cutoff <250 and peak height <15. Statistically significant differences were computed by Student's *t*-test, and the significant level was set at *P*-value $=0.01$. Only proteins with spot volumes consistently different in all replicates were considered differentially expressed.

Protein identification by matrix-assisted laser desorption/ionization time-of-flight (TOF)/ToF mass spectrometry: Proteins were identified by matrix-assisted laser desorption/ionization-TOF utilizing the method previously described.[58]

Conflict of Interest

The authors declare no conflict of interest.

Acknowledgements. This work is supported by grants to F Chiaradonna from Italian Government (FAR), Italian Ministry of Education, University and Research, MIUR (PRIN 2008, 2008P8BLNF) and by SysBioNet a MIUR grant for the Italian Roadmap of European Strategy Forum on Research Infrastructures (ESFRI). LA and CG have been partially supported by SysBioNet a MIUR grant for the Italian Roadmap of ESFRI. RP has been supported by fellowships by MIUR (Fondo Giovani 2008) and SysBioNet. We thank Neil Campbell for English editing. FC thanks his late mother for her help, support and encouragement given to him throughout her life.

1. Hanahan D, Weinberg RA. Hallmarks of cancer: the next generation. *Cell Mar* 2011; **144**: 646–674.
2. Alberghina L, Gaglio D, Gelfi C, Moresco RM, Mauri G, Bertolazzi P *et al.* Cancer cell growth and survival as a system-level property sustained by enhanced glycolysis and mitochondrial metabolic remodeling. *Front Physio* 2012; **3**: 362.
3. Chiaradonna F, Moresco RM, Airoldi C, Gaglio D, Palorini R, Nicotra F *et al.* From cancer metabolism to new biomarkers and drug targets. *Biotechnol Adv* 2011; **30**: 30–51.
4. DeBerardinis RJ, Lum JJ, Hatzivassiliou G, Thompson CB. The biology of cancer: metabolic reprogramming fuels cell growth and proliferation. *Cell Metab* 2008; **7**: 11–20.
5. Hsu PP, Sabatini DM. Cancer cell metabolism: Warburg and beyond. *Cell* 2008; **134**: 703–707.
6. Jones RG, Thompson CB. Tumor suppressors and cell metabolism: a recipe for cancer growth. *Genes Dev* 2009; **23**: 537–548.
7. Lu J, Sharma LK, Bai Y. Implications of mitochondrial DNA mutations and mitochondrial dysfunction in tumorigenesis. *Cell Res* 2009; **19**: 802–815.
8. Pelicano H, Martin DS, Xu RH, Huang P. Glycolysis inhibition for anticancer treatment. *Oncogene* 2006; **25**: 4633–4646.
9. Baracca A, Chiaradonna F, Sgarbi G, Solaini G, Alberghina L, Lenaz G. Mitochondrial Complex I decrease is responsible for bioenergetic dysfunction in K-ras transformed cells. *Biochim Biophys Acta* 2010; **1797**: 314–323.
10. Chiaradonna F, Sacco E, Manzoni R, Giorgio M, Vanoni M, Alberghina L. Ras-dependent carbon metabolism and transformation in mouse fibroblasts. *Oncogene* 2006; **25**: 5391–5404.
11. Palorini R, De Rasmo D, Gaviraghi M, Sala Danna L, Signorile A, Cirulli C *et al.* Oncogenic K-ras expression is associated with derangement of the cAMP/PKA pathway and forskolin-reversible alterations of mitochondrial dynamics and respiration. *Oncogene* 2013; **32**: 352–362.
12. Caro-Maldonado A, Tait SW, Ramirez-Peinado S, Ricci JE, Fabregat I, Green DR *et al.* Glucose deprivation induces an atypical form of apoptosis mediated by caspase-8 in Bax-, Bak-deficient cells. *Cell Death Differ* 2010; **17**: 1335–1344.
13. El Mjiyad N, Caro-Maldonado A, Ramirez-Peinado S, Munoz-Pinedo C. Sugar-free approaches to cancer cell killing. *Oncogene* 2011; **30**: 253–264.
14. Yuneva M, Zamboni N, Oefner P, Sachidanandam R, Lazebnik Y. Deficiency in glutamine but not glucose induces MYC-dependent apoptosis in human cells. *J Cell Biol* 2007; **178**: 93–105.
15. Bossu P, Vanoni M, Wanke V, Cesaroni MP, Tropea F, Melillo G *et al.* A dominant negative RAS-specific guanine nucleotide exchange factor reverses neoplastic phenotype in K-ras transformed mouse fibroblasts. *Oncogene* 2000; **19**: 2147–2154.
16. Gaglio D, Metallo CM, Gameiro PA, Hiller K, Danna LS, Balestrieri C *et al.* Oncogenic K-Ras decouples glucose and glutamine metabolism to support cancer cell growth. *Mol Syst Biol* 2011; **7**: 523.
17. Ma Y, Hendershot LM. The unfolding tale of the unfolded protein response. *Cell* 2001; **107**: 827–830.
18. Ron D, Walter P. Signal integration in the endoplasmic reticulum unfolded protein response. *Nat Rev Mol Cell Biol* 2007; **8**: 519–529.
19. Tabas I, Ron D. Integrating the mechanisms of apoptosis induced by endoplasmic reticulum stress. *Nat Cell Biol* 2011; **13**: 184–190.
20. McClain DA. Hexosamines as mediators of nutrient sensing and regulation in diabetes. *J Diabetes Complications* 2002; **16**: 72–80.
21. Slawson C, Copeland RJ, Hart GW. O-GlcNAc signaling: a metabolic link between diabetes and cancer? *Trends Biochem Sci* 2010; **35**: 547–555.
22. Xi H, Kurtoglu M, Liu H, Wangpaichitr M, You M, Liu X *et al.* 2-Deoxy-D-glucose activates autophagy via endoplasmic reticulum stress rather than ATP depletion. *Cancer Chemother Pharmacol* 2011; **67**: 899–910.
23. Sage AT, Walter LA, Shi Y, Khan MI, Kaneto H, Capretta A *et al.* Hexosamine biosynthesis pathway flux promotes endoplasmic reticulum stress, lipid accumulation, and inflammatory gene expression in hepatic cells. *Am J Physiol Endocrinol Metab* 2009; **298**: E499–E511.
24. Buse MG. Hexosamines, insulin resistance, and the complications of diabetes: current status. *Am J Physiol Endocrinol Metab* 2006; **290**: E1–E8.
25. Sax JK, Fei P, Murphy ME, Bernhard E, Korsmeyer SJ, El-Deiry WS. BID regulation by p53 contributes to chemosensitivity. *Nat Cell Biol* 2002; **4**: 842–849.
26. Weber SU, Schewe JC, Lehmann LE, Muller S, Book M, Klaschik S *et al.* Induction of Bim and Bid gene expression during accelerated apoptosis in severe sepsis. *Crit Care* 2008; **12**: R128.
27. Kitao Y, Ozawa K, Miyazaki M, Tamatani M, Kobayashi T, Yanagi H *et al.* Expression of the endoplasmic reticulum molecular chaperone (ORP150) rescues hippocampal neurons from glutamate toxicity. *J Clin Invest* 2001; **108**: 1439–1450.
28. Ozawa K, Kuwabara K, Tamatani M, Takatsuji K, Tsukamoto Y, Kaneda S *et al.* 150-kDa oxygen-regulated protein (ORP150) suppresses hypoxia-induced apoptotic cell death. *J Biol Chem* 1999; **274**: 6397–6404.
29. Scheuner D, Song B, McEwen E, Liu C, Laybutt R, Gillespie P *et al.* Translational control is required for the unfolded protein response and *in vivo* glucose homeostasis. *Mol Cell* 2001; **7**: 1165–1176.
30. Hart LS, Cunningham JT, Datta T, Dey S, Tameire F, Lehman SL *et al.* ER stress-mediated autophagy promotes Myc-dependent transformation and tumor growth. *J Clin Invest* 2012; **122**: 4621–4634.
31. Ozcan U, Yilmaz E, Ozcan L, Furuhashi M, Vaillancourt E, Smith RO *et al.* Chemical chaperones reduce ER stress and restore glucose homeostasis in a mouse model of type 2 diabetes. *Science* 2006; **313**: 1137–1140.
32. Hetz C. The unfolded protein response: controlling cell fate decisions under ER stress and beyond. *Nat Rev Mol Cell Biol* 2012; **13**: 89–102.
33. Gorman AM, Healy SJ, Jager R, Samali A. Stress management at the ER: regulators of ER stress-induced apoptosis. *Pharmacol Ther* 2012; **134**: 306–316.
34. Jager R, Bertrand MJ, Gorman AM, Vandenabeele P, Samali A. The unfolded protein response at the crossroads of cellular life and death during endoplasmic reticulum stress. *Biol Cell* 2012; **104**: 259–270.
35. Urano F, Wang X, Bertolotti A, Zhang Y, Chung P, Harding HP *et al.* Coupling of stress in the ER to activation of JNK protein kinases by transmembrane protein kinase IRE1. *Science* 2000; **287**: 664–666.
36. Bennett BL, Sasaki DT, Murray BW, O'Leary EC, Sakata ST, Xu W *et al.* SP600125, an anthrapyrazolone inhibitor of Jun N-terminal kinase. *Proc Natl Acad Sci USA* 2001; **98**: 13681–13686.
37. Romero-Fernandez W, Borroto-Escuela DO, Alea MP, Garcia-Mesa Y, Garriga P. Altered trafficking and unfolded protein response induction as a result of M3 muscarinic receptor impaired N-glycosylation. *Glycobiology* 2011; **21**: 1663–1672.
38. Mitra N, Sinha S, Ramya TN, Surolia A. N-linked oligosaccharides as outfitters for glycoprotein folding, form and function. *Trends Biochem Sci* 2006; **31**: 156–163.
39. Wellen KE, Lu C, Mancuso A, Lemons JM, Ryczko M, Dennis JW *et al.* The hexosamine biosynthetic pathway couples growth factor-induced glutamine uptake to glucose metabolism. *Genes Dev* 2010; **24**: 2784–2799.
40. Palorini R, Simonetto T, Cirulli C, Chiaradonna F. Mitochondrial complex I inhibitors and forced oxidative phosphorylation synergize in inducing cancer cell death. *Int J Cell Biol* 2013; **2013**: 243876.
41. Graham NA, Tahmasian M, Kohli B, Komisopoulou E, Zhu M, Vivanco I *et al.* Glucose deprivation activates a metabolic and signaling amplification loop leading to cell death. *Mol Syst Biol* 2012; **8**: 589.
42. Chiaradonna F, Gaglio D, Vanoni M, Alberghina L. Expression of transforming K-Ras oncogene affects mitochondrial function and morphology in mouse fibroblasts. *Biochim Biophys Acta* 2006; **1757**: 1338–1356.
43. Rutkowski DT, Kaufman RJ. That which does not kill me makes me stronger: adapting to chronic ER stress. *Trends Biochem Sci* 2007; **32**: 469–476.
44. Marciniak SJ, Yun CY, Oyadomari S, Novoa I, Zhang Y, Jungreis R *et al.* CHOP induces death by promoting protein synthesis and oxidation in the stressed endoplasmic reticulum. *Genes Dev* 2004; **18**: 3066–3077.
45. Novoa I, Zeng H, Harding HP, Ron D. Feedback inhibition of the unfolded protein response by GADD34-mediated dephosphorylation of eIF2alpha. *J Cell Biol* 2001; **153**: 1011–1022.

46. van Huizen R, Martindale JL, Gorospe M, Holbrook NJ. P58IPK, a novel endoplasmic reticulum stress-inducible protein and potential negative regulator of eIF2alpha signaling. *J Biol Chem* 2003; **278**: 15558–15564.
47. Ohoka N, Yoshii S, Hattori T, Onozaki K, Hayashi H. TRB3, a novel ER stress-inducible gene, is induced via ATF4-CHOP pathway and is involved in cell death. *EMBO J* 2005; **24**: 1243–1255.
48. Du K, Herzig S, Kulkarni RN, Montminy M. TRB3: a tribbles homolog that inhibits Akt/PKB activation by insulin in liver. *Science* 2003; **300**: 1574–1577.
49. Anelli T, Bergamelli L, Margittai E, Rimessi A, Fagioli C, Malgaroli A *et al.* Ero1alpha regulates Ca(2+) fluxes at the endoplasmic reticulum-mitochondria interface (MAM). *Antioxid Redox Signal* 2012; **16**: 1077–1087.
50. Li G, Mongillo M, Chin KT, Harding H, Ron D, Marks AR *et al.* Role of ERO1-alpha-mediated stimulation of inositol 1,4,5-triphosphate receptor activity in endoplasmic reticulum stress-induced apoptosis. *J Cell Biol* 2009; **186**: 783–792.
51. Bassik MC, Scorrano L, Oakes SA, Pozzan T, Korsmeyer SJ. Phosphorylation of BCL-2 regulates ER Ca2+ homeostasis and apoptosis. *EMBO J* 2004; **23**: 1207–1216.
52. Nishitoh H, Matsuzawa A, Tobiume K, Saegusa K, Takeda K, Inoue K *et al.* ASK1 is essential for endoplasmic reticulum stress-induced neuronal cell death triggered by expanded polyglutamine repeats. *Genes Dev* 2002; **16**: 1345–1355.
53. Wei Y, Sinha S, Levine B. Dual role of JNK1-mediated phosphorylation of Bcl-2 in autophagy and apoptosis regulation. *Autophagy* 2008; **4**: 949–951.
54. Ying H, Kimmelman AC, Lyssiotis CA, Hua S, Chu GC, Fletcher-Sananikone E *et al.* Oncogenic Kras maintains pancreatic tumors through regulation of anabolic glucose metabolism. *Cell* 2012; **149**: 656–670.
55. Guillaumond F, Leca J, Olivares O, Lavaut MN, Vidal N, Berthezene P *et al.* Strengthened glycolysis under hypoxia supports tumor symbiosis and hexosamine biosynthesis in pancreatic adenocarcinoma. *Proc Natl Acad Sci USA* 2013; **110**: 3919–3924.
56. Pulciani S, Santos E, Long LK, Sorrentino V, Barbacid M. ras gene Amplification and malignant transformation. *Mol Cell Biol* 1985; **5**: 2836–2841.
57. Irizarry RA, Hobbs B, Collin F, Beazer-Barclay YD, Antonellis KJ, Scherf U *et al.* Exploration, normalization, and summaries of high density oligonucleotide array probe level data. *Biostatistics* 2003; **4**: 249–264.
58. Vigano A, Vasso M, Caretti A, Bravata V, Terraneo L, Fania C *et al.* Protein modulation in mouse heart under acute and chronic hypoxia. *Proteomics* 2011; **11**: 4202–4217.

Supplementary Information accompanies this paper on Cell Death and Disease website (http://www.nature.com/cddis)